Solution Synthesis and Characterization of Quantum Confined Ge Nanoparticles

Boyd R. Taylor and Susan M. Kauzlarich*

Department of Chemistry, University of California, One Shields Avenue, Davis, California 95616-5295

Gildardo R. Delgado and Howard W. H. Lee

Lawrence Livermore National Laboratory, P.O. Box 808, Livermore, California 94551

Received April 12, 1999. Revised Manuscript Received July 12, 1999

A solution synthesis of crystalline Ge nanoparticles (nc-Ge) is reported. The metathesis reaction of NaGe with excess $GeCl_4$ in glyme solvents produces nc-Ge. Metathesis reactions between KGe and excess $GeCl_4$ or $GeCl_2$:(dioxane) in glyme and Mg_2Ge and excess $GeCl_4$ in diglyme and triglyme were also investigated. The surface of these nanoparticles is terminated with alkyl groups by reaction with alkyl Li and Grignard reagents. The alkyl-terminated crystalline Ge nanoparticles (R̂-nc-Ge) were characterized by Fourier transform infrared spectroscopy, high-resolution transmission electron microscopy, powder X-ray diffraction, UV−vis absorption spectroscopy, photoluminescence, and photoluminescence excitation spectroscopy. The optical properties of R̂-nc-Ge made by this method agree with predictions from quantum confinement models.

Introduction

Semiconductor nanoparticles or quantum dots are uniquely interesting systems from both theoretical and experimental viewpoints.[1] Interest in group IV nanoparticles stems from reports of efficient luminescence in these materials and the possibility of new materials for optoelectronic applications.[2−4] Our interest in nc-Ge stems from reported luminescence[5−13] and the predictions of enhanced nonlinear properties.[14−16] While there has been a great deal of work on porous Si[4,17−19] and Si nanoparticles,[20−23] there has been relatively little work on porous Ge[24] or nc-Ge. nc-Ge's have been prepared by a variety of chemical and physical methods. Chemical methods include oxidation and then reduction of doped silica xerogels,[25] hydrolysis of $GeCl_4$ in Zeolite Y followed by H_2 reduction,[26] reduction of $GeCl_4$ and $RGeCl_3$ by Na dispersion in heptane,[27,28] and reduction of $GeCl_4$ by Li naphthlide.[29] Physical methods such as chemical vapor deposition (CVD),[8,30,31] rf cosputtering of Ge and SiO_2 followed by H_2 reduction,[6,32−34] pulsed

(1) Zunger, A., Ed. *MRS Bull.* **1998**, *23*, 15−53.
(2) Brus, L. *J. Phys. Chem.* **1994**, *98*, 3575−3581.
(3) Brus, L. E. *Semiconductor Nanocrystals, Microelectronics, and Solar Cells*; Laudise, R. A., Ed.; The Robert A. Welch Foundation 39th Conference on Chemical Research, Nanophase Chemistry; Houston, TX, 1995; pp 21−28.
(4) Sailor, M. J.; Kavanagh, K. L. *Adv. Mater.* **1992**, *4*, 432.
(5) Kanemitsu, Y.; Uto, H.; Masumoto, Y.; Maeda, Y. *Appl. Phys. Lett.* **1992**, *61*, 2187−2189.
(6) Maeda, Y.; Tsukamoto, N.; Yazawa, Y.; Kanemitsu, Y.; Masumoto, Y. *Appl. Phys. Lett.* **1991**, *59*, 3168−3170.
(7) Kanemitsu, Y. *J. Non-Cryst. Solids* **1993**, *164−166*, 639−642.
(8) Dutta, A. K. *Appl. Phys. Lett.* **1996**, *68*, 1189−1191.
(9) Zacharias, M.; Bläsing, J.; Christen, J.; Veit, P.; Dietrich, B.; Bimberg, D. *Superlattices Microstruct.* **1995**, *18*, 139−145.
(10) Zacharias, M.; Christen, J.; Bläsing, J.; Bimberg, D. *J. Non-Cryst. Solids* **1996**, *198−200*, 115−118.
(11) Zacharias, M.; Fauchet, P. M. *Appl. Phys. Lett.* **1997**, *71*, 380−382.
(12) Yang, C. M.; Shchlegov, K. V.; Vahala, K. J.; Atwater, H. A. *Nucl. Instrum. Methods Phys. Res. B* **1995**, *106*, 433−437.
(13) Min, K. S.; Shcheglov, K. V.; Yang, C. M.; Atwater, H. A.; Brongersma, M. L.; Polman, A. *Appl. Phys. Lett.* **1996**, *68*, 2511−2513.
(14) Brus, L. *Appl. Phys. A.* **1991**, *53*, 465−474.
(15) Wang, Y.; Herron, N. *J. Phys. Chem.* **1991**, *95*, 525−532.
(16) Wang, Y. *Acc. Chem. Res.* **1991**, *24*, 133−139.
(17) Prokes, S. M.; Glembocki, O. J. *Mater. Chem. Phys.* **1993**, *35*, 1−10.
(18) Prokes, S. M. *J. Mater. Res.* **1996**, *11*, 305−320.
(19) Cullis, A. G.; Canham, L. T.; Calcott, P. D. J. *J. Appl. Phys.* **1997**, *82*, 909−965.
(20) Bley, R. A.; Kauzlarich, S. M.; Lee, H. W. H.; Davis, J. E. *Mater. Res. Soc. Symp. Proc.*, MRS; San Francisco, 1994; Vol. 351, pp 275−280.
(21) Bley, R. A.; Kauzlarich, S. M. *J. Am. Chem. Soc.* **1996**, *118*, 12461−12462.
(22) Bley, R. A.; Kauzlarich, S. M. *Synthesis of Silicon Nanoclusters*; Fendler, J. H., Ed.; VCH Publishers: New York, 1997; pp 101−118.
(23) Bley, R. A.; Kauzlarich, S. M. *A New Solution Phase Synthesis for Silicon Nanoclusters*; Fendler, J. H., Dekany, I., Eds.; Kluwer Academic Publishers: Netherlands, 1997; pp 467−475.
(24) Miyazaki, S.; Sakamoto, K.; Shiba, K.; Hirose, M. *Thin Solid Films* **1995**, *255*, 99−102.
(25) Carpenter, J. P.; Lukehart, C. M.; Henderson, D. O.; Mu, R.; Jones, B. D.; Glosser, R.; Stock, S. R.; Wittig, J. E.; Zhu, J. G. *Chem. Mater.* **1996**, *8*, 1268−1274.
(26) Miguez, H.; Fornes, V.; Meseguer, F.; Marquez, F.; Lopez, C. *Appl. Phys. Lett.* **1996**, *69*, 2347−2349.
(27) Heath, J. R.; LeGoues, F. K. *Chem. Phys. Lett.* **1993**, *208*, 263−268.
(28) Heath, J. R.; Shiang, J. J.; Alivisatos, A. P. *J. Chem. Phys.* **1994**, *101*, 1607−1615.
(29) Kornowski, A.; Giersig, M.; Vogel, R.; Chemseddine, A.; Weller, H. *Adv. Mater.* **1993**, *5*, 634−636.
(30) Kobayashi, T.; Endoh, T.; Fukuda, H.; Shigeru, N.; Sakai, A.; Ueda, Y. *Appl. Phys. Lett.* **1997**, *71*, 1195−1197.
(31) Halimaoui, A.; Campidelli, Y.; Badoz, P. A.; Bensahel, D. *J. Appl. Phys.* **1995**, *78*, 3428−3430.
(32) Fujii, M.; Hayashi, S.; Yamamoto, K. *Appl. Phys. Lett.* **1990**, *57*, 2692−2694.
(33) Fujii, M.; Hayashi, S.; Yamamoto, K. *Jpn. J. Appl. Phys.* **1991**, *30*, 687−694.
(34) Fujii, M.; Wada, M.; Hayashi, S.; Yamamoto, K. *Phys. Rev. B* **1992**, *46*, 15930−15935.

10.1021/cm990203q CCC: $18.00
Published on Web 08/27/1999

laser ablation of Ge,[35] and ion implant of Ge into SiO_2 layers have also succeeded in producing Ge quantum dots.[36]

While the aforementioned techniques provide nc-Ge, they all suffer from some difficulties. Many produce nanoparticles in a matrix, which complicates both the spectroscopy and device design. Additionally, none of the techniques mentioned previously permits simultaneous control over particle size and surface termination. A formidable difficulty of the CVD or sputtering methods is that they do not permit the synthesis of large amounts of nc-Ge. Addressing these difficulties calls for a synthesis that gives nanoparticles without a matrix, permits control over particle size and surface termination, and can produce large quantities of nanoparticles. Synthetic methods meeting these criteria may be derived by considering solution syntheses that have been developed in more mature areas of semiconductor nanoparticles, such as production of II−VI semiconductor nanoparticles.

The synthesis of II−VI semiconductor nanoparticles is well-established, with researchers demonstrating great control over the size and surface termination of these nanoparticles.[37,38] While the synthesis of III−V semiconductor nanoparticles is not as well-established, their solution synthesis has recently been demonstrated.[39−41] Researchers recently have had great success in synthesizing InP quantum dots using colloidal chemistry,[42] and demonstrated quantum confinement in these quantum dots by size-selective spectroscopy.[43] Two solution syntheses of nc-Ge and quantum wires have been reported by other groups.[27−29] However, both of these methods have drawbacks. The reduction of $GeCl_4$ and $RGeCl_3$ by Na−K dispersion in heptane required heating to 270 °C for 24−48 h at high pressures to force crystallization.[27,28] The reduction of $GeCl_4$ by lithium naphthlide[29] led to an amorphous product, which required annealing with a red laser to produce crystalline nanoparticles. Additionally, neither method permits control over particle size or surface termination.

A solution synthesis which permits both control over surface termination and production of useful amounts of alkyl-terminated crystalline Si nanoparticles (R̂-nc-Si) and R̂-nc-Ge has recently been developed.[20−23,44] This paper presents more detailed work on the synthetic conditions and characterization of R̂-nc-Ge.

Experimental Section

Synthesis. All manipulations were carried out under dry N_2 or Ar gas, using a glovebox filled with N_2 or using standard Schlenk line techniques.[45] Ethylene glycol dimethyl ether (glyme) and diethylene glycol dimethyl ether (diglyme) were dried and distilled from Na−K alloy prior to use. Triethylene glycol dimethyl ether was dried and distilled from Na metal prior to use. Ge powder (99.999%, Aldrich), Na and K metal (99%, Fisher), $GeCl_4$ (99.99%, Fisher (Acros)), methylmagnesium bromide (2 M in THF, Aldrich), methyllithium (1.6 M in diethyl ether, Fisher (Acros)), octylmagnesium chloride (5 M in THF, Aldrich), butyllithium (1.6 M in hexanes, Fisher (Acros)), and HPLC grade hexanes (Aldrich) were used as received.

Synthesis of Ge Nanocrystal Colloids from NaGe. The colloidal solutions of nanoparticles were synthesized as follows: Sodium germanide (NaGe) was prepared according to a literature preparation,[46] that was modified by the addition of ∼10 molar percent excess of Na metal in order to ensure complete reaction of the Ge. Excess Na was removed by sublimation on a high-vacuum line at 300 °C for 4 h. KGe was prepared and purified in a similar manner.[47] The purity of the product was determined by powder XRD. For both Zintl salts, yield was quantitative and the powder pattern matched the powder pattern calculated from single-crystal refinement data.[46,47] In the glovebox, purified NaGe (0.250−0.260 g, 2.6 mmol) or KGe (0.100−0.110 g, 0.90 mmol) was added to a silonated[48] 250-mL three-neck round-bottom flask. Approximately 150 mL of diglyme, glyme, or triglyme was added to the NaGe or KGe powder using a cannula. The mixture of NaGe or KGe and glyme solvent was heated and allowed to reflux for 12 h, and $GeCl_4$ was added in a 3-fold excess to the resulting gray suspension. The reaction mixture was allowed to reflux for 4−120 h in diglyme; reflux times of 8−24 h were typical, with longer reflux times used in attempts to produce larger nanoparticles. Reactions carried out in glyme were allowed to reflux for 24 h after the addition of $GeCl_4$; the effect of reflux time was not investigated in glyme, since this solvent did not appear to support the reaction well. Reactions in triglyme were allowed to react for 0.5−4 h after the addition of $GeCl_4$. The reaction mixture in triglyme changed color to deep gold within 5 min of adding the $GeCl_4$, while reaction mixtures in diglyme changed from gray to bright yellow and clarified over a 3−4 h interval. The reaction mixture in glyme did not change in color or clarify even after refluxing for 24 h. A white precipitate formed as the reaction continued; this precipitate was presumably sodium or potassium chloride. At longer reflux times, in excess of 24 h for the reaction in diglyme, the solution turned brown and opaque. The excess $GeCl_4$ was removed by evacuation through a trap cooled with liquid N_2. For reactions carried out in glyme, all of the solvent was removed since the boiling points of $GeCl_4$ (84 °C) and glyme (83−84 °C) are the same. It was found that addition of a 3-fold excess of $GeCl_4$ was necessary to achieve the desired results; addition of a stoichiometric amount of $GeCl_4$ resulted in an incomplete reaction, while using a larger excess led to the formation of large amounts of molecular species and other side-products. Why an excess of $GeCl_4$ was required for the reaction to run to completion is not yet known. Interestingly, despite the 3-fold excess of $GeCl_4$ used in the reaction, only small amounts of $GeCl_4$ were removed even under prolonged evacuation and gentle heating. Excess alkyllithium or Grignard reagent was added by airtight syringe and the mixture stirred overnight at room temperature. More white precipitate was observed upon addition of the alkyllithium or Grignard reagent. After 12−24 h, excess alkyllithium or Grignard reagent was neutralized by the addition of ∼50 mL of 20 MΩ deionized water.

Synthesis of Ge Nanocrystal Colloids from Mg_2Ge. The colloidal solutions were prepared as follows: Mg_2Ge was prepared from a literature preparation and used without further purification.[49] The yield was quantitative and the

(35) Ngiam, S.-T.; Jensen, K. F.; Kolenbrander, K. D. *J. Appl. Phys.* **1994**, *76*, 8201−8203.
(36) Zhu, J. G.; White, C. W.; Budai, J. D.; Withrow, S. P.; Chen, Y. *J. Appl. Phys.* **1995**, *78*, 4386-4389.
(37) Alivisatos, A. P. *J. Phys. Chem.* **1996**, *100*, 13226−13239.
(38) Weller, H. *Angew. Chem., Int. Ed. Engl.* **1993**, *32*, 41−53.
(39) Kher, S. S.; Wells, R. L. *Chem. Mater.* **1994**, *6*, 2056−2062.
(40) Kher, S. S.; Wells, R. L. *Mater. Res. Soc. Sym. Proc.* **1994**, *351*, 293−298.
(41) Wells, R. L.; Janik, J. F. *Eur. J. Solid State Inorg. Chem.* **1996**, *33*, 1079−1090.
(42) Guzelian, A. A.; Katari, J. E. B.; Kadavanich, A. V.; Banin, U.; Hamad, K.; Juban, E.; Alivisatos, A. P.; Wolters, R. H.; Arnold, C. C.; Heath, J. R. *J. Phys. Chem.* **1996**, *100*, 7212−7219.
(43) Micic, O. I.; Cheong, H. M.; Fu, H.; Zunger, A.; Sprague, J. R.; Mascarenhas, A.; Nozik, A. J. *J. Phys. Chem. B* **1997**, *101*, 4904−4912.
(44) Taylor, B. R.; Kauzlarich, S. M.; Lee, H. W. H.; Delgado, G. R. *Chem. Mater.* **1998**, *10*, 22−24.
(45) Shriver, D. F.; Drezdzon, M. A. *The Manipulation of Air-Sensitive Compounds*; Wiley-Interscience: New York, 1986.
(46) Schäfer, R.; Klemm, W. *Z. Anorg. Allg. Chem.* **1961**, *312*, 214−220.
(47) Busmann, V. E. *Z. Anorg. Allg. Chem.* **1961**, *313*, 90−106.

powder XRD of the Mg_2Ge produced matched the powder pattern calculated from single-crystal XRD data. Although Mg_2Ge is not air-sensitive, all manipulations were carried out in a glovebox filled with dry N_2 or using standard Schlenk line techniques under dry Ar. In the glovebox, Mg_2Ge (0.250−0.260 g, 2.1 mmol) was added to a silonated 250-mL three-neck round-bottom flask. Approximately 150 mL of dry diglyme or triglyme was added to the flask by cannula. Reactions between Mg_2Ge and $GeCl_4$ were not investigated in glyme. The resulting suspension of Mg_2Ge in diglyme or triglyme was heated to reflux with stirring overnight. A 3-fold excess of $GeCl_4$ was added to the suspension by airtight syringe. The mixture was allowed to react for 0.5−4 h after the addition of $GeCl_4$. Reactions in triglyme were much faster than in diglyme. The reaction mixture clarified and changed from dark gray to gold or orange over a period of several minutes rather than 2−4 h for reactions in diglyme. The excess $GeCl_4$ was removed from the reaction mixture by evacuation of the warm suspension through a trap cooled by liquid N_2. Similar to reactions between $GeCl_4$ and NaGe or KGe, very little of the $GeCl_4$ is collected on evacuation; no reactions were attempted at different stoichiometries of $GeCl_4$. Excess methyllithium, butyllithium, or octylmagnesium bromide solution was added by airtight syringe, and the suspension was allowed to react for 12−24 h. Additional white precipitate formed upon the addition of the alkyllithium or Grignard reagent, presumably LiCl or MgClBr, since no GeO_2 was found in any of the reaction products. The excess alkyllithium or Grignard reagent was quenched by the addition of 50 mL of 20 MΩ deionized water.

Separation and Purification. The reaction mixture was transferred to a 500-mL separatory funnel, 50 mL of hexane was added, and salts were extracted with deionized water. The nanoparticles formed a deep yellow to deep red colloid in hexane, with the color varying roughly according to particle size and concentration. This colloid was rinsed repeatedly with deionized water to remove the last traces of the salts. When samples were terminated with Grignard reagents, the reaction was rinsed with 1 M HCl to remove any $Mg(OH)_2$ formed on quenching the reaction mixture with water. A tan precipitate formed with the first two water rinses of the deep red hexane colloid, which was not soluble in dilute HCl. This precipitate was removed by filtering the reaction mixture through a Whatman #1 filter paper. The extraction process was repeated, and the hexane layers of each extract were combined. The combined hexane extracts were concentrated using a rotary evaporator, which gave a deep red viscous colloid. So long as this colloid was not taken to dryness, it was readily resuspended in hexane or other solvents. Colloids prepared from M̂e-nc-Ge formed more stable colloids in polar solvents such as methanol, while B̂u-nc-Ge and Ôc-nc-Ge formed more stable colloids in less polar solvents such as hexane and toluene.

Characterization. A Mattson Galaxy 3000 FTIR spectrophotometer was used to perform IR spectroscopy on the dried colloids. Each colloid was dried on a CsI plate, and heated at 110 °C for 2 h to remove the solvent, and then cooled in a desiccator before examination; a blank CsI plate was examined before each sample. To obtain FTIR spectra of dried powders, they were pressed into a CsI pellet; a blank CsI pellet was examined before each sample. High-resolution transmission electron microscopy (HRTEM) of the colloids was performed with a Phillips CM200 field emission gun TEM operating at 200 keV, with an information limit of 1.7 Å and a point-to point resolution of 2.4 Å. A 10−15 μL aliquot of the colloid was pipetted 5 μL at a time onto a lacey carbon substrate on a 300 mesh Cu TEM grid and dried. All HRTEM images were acquired digitally using Digital Micrograph software from Gatan, Inc.; the digitized files were rotationally filtered using an algorithm available from the National Center for Electron Microscopy at Lawrence Berkeley National Laboratory. No further image processing was necessary or desirable, as it led to obvious artifacts in the images. The colloids produced were diluted with HPLC grade hexane and examined with a Hewlett-Packard HP8452A UV−vis spectrophotometer. A blank of pure solvent was examined before every sample. The photoluminescence spectra of these colloids were acquired on Perkin-Elmer LS50B and Shimadzu RF-5301PC spectrofluorophotometers. A slit width of 2.5 nm was used for both the excitation and emission monochromators with the LS50B; spectra were collected on the RF-5301PC with slit widths of 3.0 nm. The photoluminescence emission spectra are corrected for variations in excitation intensity by the instrument. The colloids were diluted as necessary, and pure solvent was spectroscopically examined before acquiring photoluminescence spectra. Additionally, the colloids produced were heated to remove any molecular species and the dried microcrystalline powders were examined by powder X-ray diffraction (XRD) with a Siemens D500 diffractometer using Cu Kα radiation.

Results and Discussion

The reaction between NaGe, KGe, or Mg_2Ge and $GeCl_4$ in refluxing diglyme or triglyme is nearly quantitative. The reaction, as judged by the change in reaction mixture from a gray opaque suspension to a clear yellow solution, runs to completion. The lack of any GeO_2, NaOH, KOH, or any precipitate resembling the Zintl salts used as starting materials also supports the extent of reaction. Diglyme and triglyme appear to support the reaction better than glyme. None of these Zintl salts will dissolve completely in glyme, even after the addition of excess $GeCl_4$ and refluxing for 24 h. The reactions in glyme did not turn yellow or clarify during the reaction, unlike reactions in diglyme and triglyme. Additionally, Ge nanoparticles produced by reaction in glyme have a larger average particle size, and the yield of crystalline nanoparticles is much lower. There is no noticeable difference between the reaction of KGe or NaGe with $GeCl_4$, and the majority of reactions were investigated using NaGe. Various reaction conditions have been investigated. Typically, the NaGe or KGe was stirred in refluxing in diglyme (bp = 162 °C) overnight prior to the addition of $GeCl_4$. While this stirring overnight did form a better suspension and permit the reaction to occur more quickly, it was not vital to the reaction. The reaction between NaGe or KGe, and $GeCl_4$ was typically carried out at a 3-fold excess of $GeCl_4$; some reactions were carried out on stoichiometry, but excess $GeCl_4$ was found necessary for the NaGe or KGe to completely dissolve in digylme. Reactions carried out with a 10-fold excess of $GeCl_4$ produced large amounts of intractable side-products. Differing stoichiometric excesses of $GeCl_4$ were not investigated in reactions with Mg_2Ge. As a reagent, Mg_2Ge behaved similarly to NaGe and KGe, suggesting that any germanide is suitable for this reaction. Reaction with both alkyllithium and Grignard reagents terminate the surface of the nanoparticles; methyl and butyl groups were used for alkylithium reagents, methyl and octyl groups were used for Grignard reagents. The R̂-nc-Ge are unreactive to both air and water, despite the reactivity of NaGe, KGe and $GeCl_4$. Before drying, the colloid formed was quite stable; it could stand without any precipitate formation for several weeks. The colloid formed by resuspending the dried, purified R̂-nc-Ge was not as stable as the original colloid, but was still sufficiently stable that a precipitate did not form for several days from the resuspended nanoparticles. Estimating solely by the ratio of the weight of the dried nanoparticles to the Zintl salt used as starting material, the yield of the reaction in diglyme was ∼40%, with reactions in glyme and triglyme producing smaller and larger yields, respec-

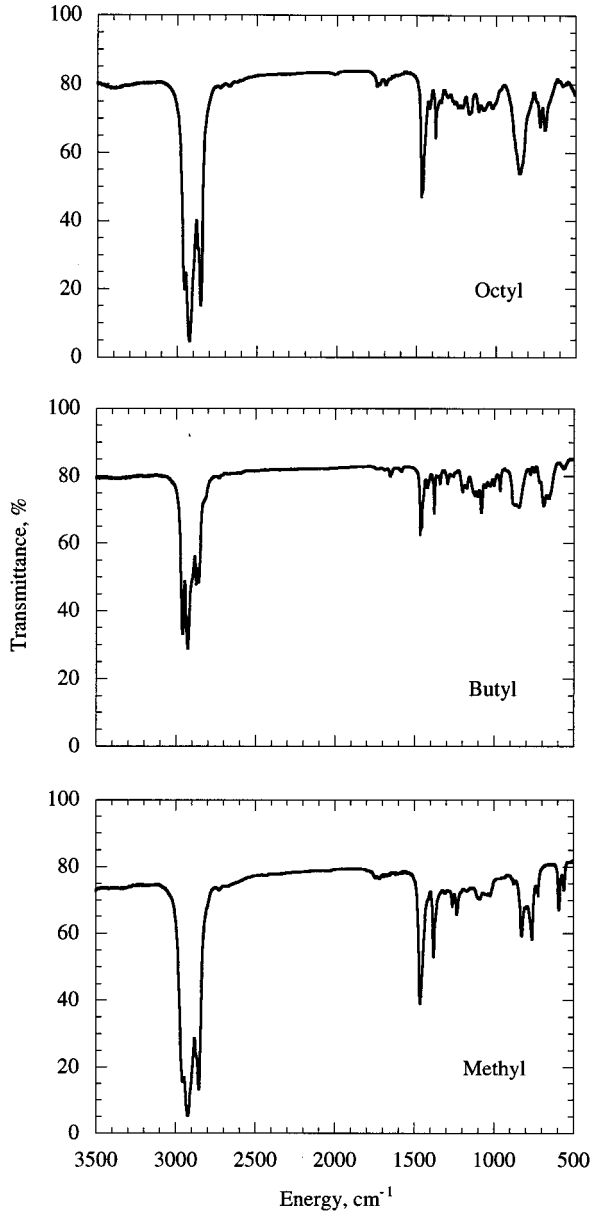

Figure 1. FTIR spectra of dried films of methyl-, butyl-, and octyl-terminated Ge nanoparticles.

tively. At the present time, the question of yields based on weights needs to be explored further, for reasons discussed in the XRD characterization.

FTIR spectra of the dried colloids demonstrate the surface termination of these nanoparticles by alkyl groups for both RLi and RMgBr. Three different terminating groups have been used; methyl, butyl, and octyl. For R = methyl, both the Li reagent and Grignard reagent were used. The resulting surface termination was identical in both cases, based on the FTIR spectra. For R = butyl and octyl, the Li reagent and the Grignard reagent were used, respectively. RLi is preferred as a terminating reagent since LiOH dissolves more easily than $Mg(OH)_2$ in H_2O. Figure 1 shows the FTIR for the three different terminating groups. The three peaks at 2955, 2924, and 2853 cm^{-1} fall where expected for the C−H stretches of methyl and methylene groups. The peaks at 1376 and 1456 cm^{-1} are at the positions expected for the symmetric and asymmetric bends of the methyl group, respectively. The Ge−C stretch is typically seen at 830 cm^{-1}, although the Ge−C stretch for the M̂e-nc-Ge is at 860 cm^{-1}. The Ge−O stretch is typically seen at 870−910 cm^{-1}; since the Ge−O stretch is broad and intense some overlap of the two bands is expected. The presence of the methylene peak in the FTIR suggests that methyl group loses a proton and bonds to the Ge surface as a methylene group in the M̂e-nc-Ge. It is possible that there is a mixture of methyl and methylene on the surface of the nanoparticles. At the least, the alkyl termination prevents oxidation of the particles and provides a stable passivation layer. The spectra of the dried colloids were compared to both published spectra for the Ge tetraalkyls[50,51] and GeO_2.[52] In every case, the Ge−C stretch is seen, and the Ge−O stretch is absent. This does not rule out small amounts of surface oxide, but as FTIR is more sensitive to Ge−O stretches than Ge−C stretches, it is unlikely that significant oxide is present. The Ge−C bonds are quite stable in these colloids; the colloids have been heated to 110 °C in air for several days without producing sufficient surface oxide to detect by FTIR. This is in agreement with early work on Ge tetraalkyls,[53] which demonstrated that they can be heated in air to more than 300 °C without decomposition. In fact, pyrolysis takes place with Ge tetraalkyls at practical rates only above 400 °C.[54]

The hexane colloid was dried on a Cu TEM grid coated with a lacey carbon film and examined by HRTEM. The HRTEM image in Figure 2 shows that the majority of the small particles seen in the TEM are crystalline. The lattice plane imaged is typically Ge {111}, although {200} sometimes is resolved. The measured *d* spacings were ~3.27 Å for {111}, and 2.00 Å for {200}; these *d* spacings fit bulk Ge within the accuracy of measurement. Since the {111} planes are both the widest spacing and most probable in the diamond cubic lattice, this is as expected. Selected area electron diffraction (SAED) was also performed on these samples; the diffraction pattern obtained from the R̂-nc-Ge matched the expected *d* spacings for bulk Ge, with the (111), (220), and (311) reflections all seen, with *d* spacings of 3.27, 2.00, and 1.71 Å, respectively. The fast Fourier transform (FFT) of the HRTEM image of a single nanoparticle along the [110] zone axis, shown in Figure 3, revealed the expected pseudohexagonal symmetry of the {111} face of a diamond-cubic crystal. While the previous report of this synthetic method stated that a log-normal size distribution is obtained,[44] repeated measurements of size distribution of several samples by HRTEM have shown both log-normal and Gaussian distributions. Figure 4 shows the size distribution of the methyl-, butyl-, and octyl-terminated samples deduced from TEM images. This variability of the shape of the

(48) Diaz, A. F. *Some Studies With Chemically Modified Surfaces*, 1st ed.; Leyden, D. E., Collins, W. T., Eds.; Gordon and Breach: New York, 1980; Vol. 7, pp 135−157.
(49) Klemm, W.; Westlinning, Z. *Z. Anorg. Chem.* **1941**, *245*, 365−380.
(50) Fuchs, R.; Moore, L.; Miles, D.; Gilman, H. *J. Org. Chem.* **1956**, *21*, 1113−1117.
(51) Lippincott, E. R.; Tobin, M. C. *J. Am. Chem. Soc.* **1953**, *75*, 4141−4147.
(52) Galeener, F. L.; Leadbetter, A. J.; Stringfellow, M. W. *Phys. Rev. B* **1982**, *27*, 1052−1077.
(53) Winkler, C. *J. Prakt. Chem.* **1887**, *36*, 177−209.
(54) Geddes, R. L.; Mack, E. *J. Am. Chem. Soc.* **1930**, *52*, 4372−4380.

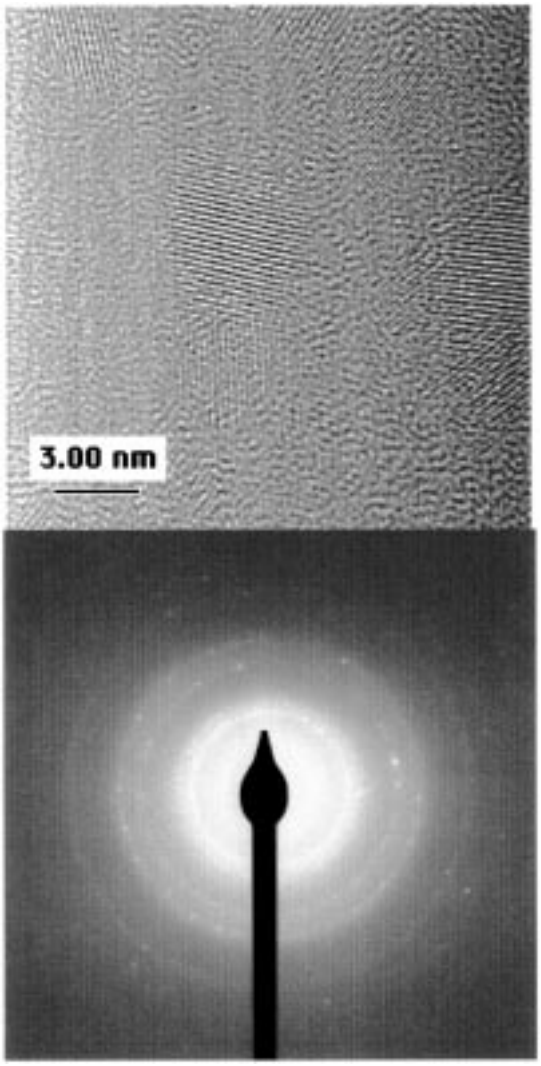

Figure 2. (a) A high-resolution micrograph of several methyl-terminated Ge nanoparticles. The wider lattice fringes are from {111}, with a *d* spacing of 3.27 Å, while the narrower lattice fringes are from {220}, with a *d* spacing of 2.00 Å. (b) SAED of numerous Ge nanoparticles prepared from Mg_2Ge. Ge {220}, {311}, and {400} are seen clearly; Ge {111} is present, but obscured by the central spot of the transmitted beam.

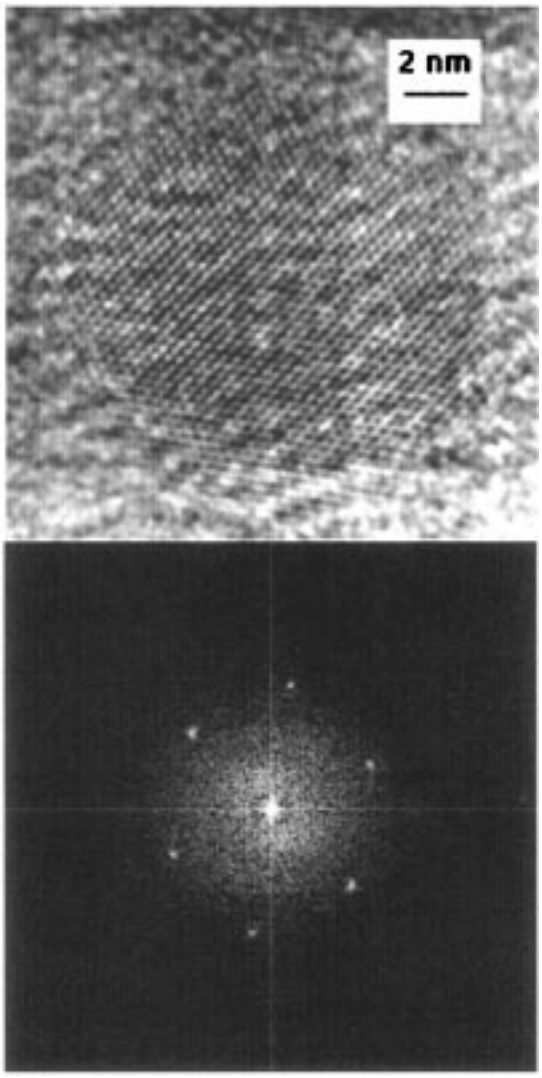

Figure 3. (a) The high-resolution image of the {111} face of a single Ge nanoparticle of ~15 nm in diameter. (b) The fast Fourier transform of the image demonstrates the pseudo-hexagonal symmetry of the {111} face of Ge.

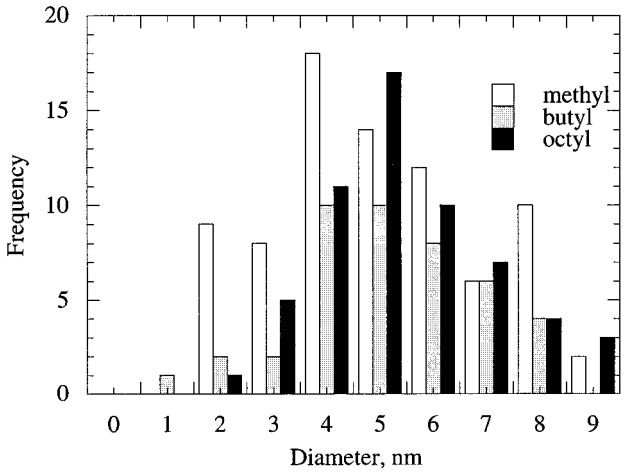

Figure 4. Size distributions of methyl-, butyl-, and octyl-terminated Ge nanoparticles. These histograms demonstrate the size distributions of the samples as prepared, before any further size separation. All three samples have mean diameters of 6.2−6.5 nm.

size distribution seen in these samples is most likely due to the handling they received during HRTEM sample preparation and the slight differences in the HRTEM specimens as prepared. The most likely case is that all samples have an approximately Gaussian size distribution, but the smallest particles are difficult to resolve against the background of the holey carbon support film.

Since the size distribution obtained from HRTEM characterization suffers from several difficulties, powder XRD was also used to measure the size of the nanoparticles. Heating the tan material from the initial purification of the colloid at 600 °C for 8 h under vacuum removed any alkyl termination, permitting characterization by powder XRD, but did not cause the nanoparticles produced to grow in size significantly. The sample suffered a 58% weight loss during the heating, most of which appeared to be the surface terminating alkyl, residual solvent, and molecular species. After heating, it was no longer possible to suspend the nanoparticles in common solvents. The broadened (111), (220), and (311) reflections from a heated sample of Me-nc-Ge are

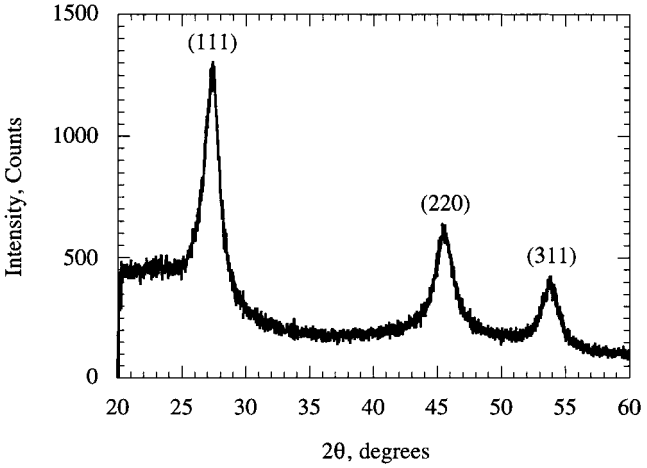

Figure 5. Powder XRD of methyl-terminated Ge nanoparticles prepared in triglyme, then heated to 600 °C for 8 h.

Table 1. Summary of the Effects of Relative Concentration of Starting Materials and Solvent Used on the Mean Size of Ge Nanoparticles

solvent	surface termination	relative concentration	mean size, nm (standard deviation)
glyme	methyl	1.0	8−10
diglyme	methyl	2.5	6.9 (3.6)
diglyme	octyl	2.5	6.2 (2.6)
diglyme	octyl	2.5	6.9 (3.0)
triglyme	methyl	5.0	4.5 (3.0)

seen in Figure 5. The size of the heated nanoparticles was determined from the width of the reflections according to the Debye−Scherrer equation:[55]

$$B = \frac{0.9\lambda}{t \cos \theta}$$

For a broadening of ∼2.2° (fwhm) for the (111) reflection of Ge, with $\lambda = 1.5418$ Å for Cu Kα radiation, a mean diameter of approximately 4.1 nm was found for M̂e-nc-Ge produced by reaction of Mg_2Ge with $GeCl_4$ in triglyme. This is consistent with, although slightly smaller than, the mean size of 4.5 nm (Table 1), as determined by measuring the HRTEM micrographs. The nanoparticles as produced showed no well-defined reflections when heated to lower temperatures, but did show a broad peak from 2θ of 20° to 30°, suggesting poorly crystallized nanoparticles. Additionally, the broad size distributions, small particle size, and the presence of noncrystalline impurities all contribute to the very weak diffraction of the as-prepared particles.

The question of quantum confinement is an important issue of these nanoparticles. Quantum confinement results in optical properties that are highly size-dependent, e.g., smaller nanoparticles absorb and emit light at higher energies than larger nanoparticles and have larger oscillator strengths. While bulk Ge absorbs weakly in the infrared, nanoparticles produced by this method absorb strongly in the visible and ultraviolet. Figure 6 shows UV−vis absorption spectra of M̂e-nc-Ge, B̂u-nc-Ge, and Ôc-nc-Ge of ∼6.5 nm mean diameter produced in refluxing diglyme. The spectra are very similar and nearly featureless, showing an absorption

(55) Cullity, B. D. *Elements of X-ray Diffraction*; 2nd ed.; Addison-Wesley: Menlo Park, 1978.

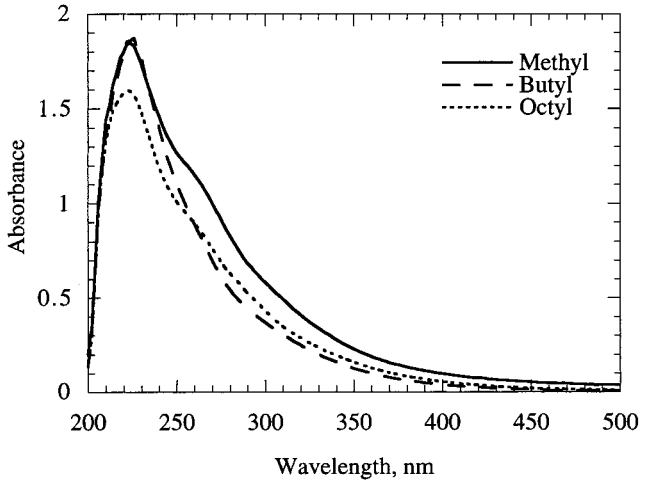

Figure 6. UV−vis absorption spectra of methyl-, butyl-, and octyl-terminated Ge nanoparticles in hexane. All spectra have similar shape and absorption onsets.

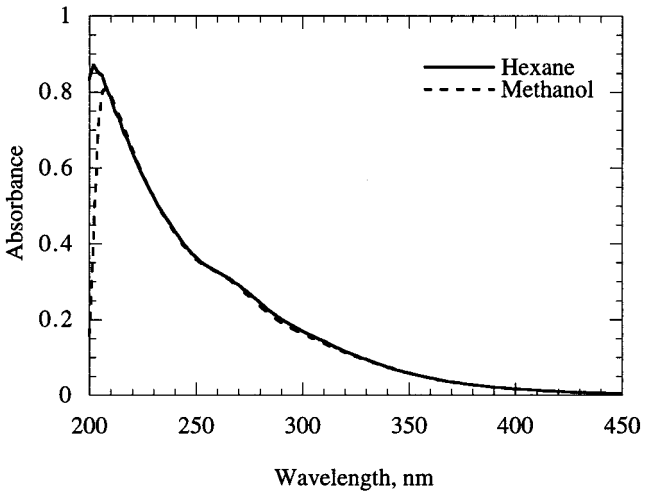

Figure 7. UV−vis absorption spectra of 6.5 nm methyl-terminated Ge nanoparticles in hexane and methanol.

onset considerably above the band gap of bulk Ge. The above band gap absorption suggests that these nanoparticles are quantum confined. The reason for this large shift in the band gap of these nanoparticles relative to bulk is not known, although it suggests a direct band gap in these nanoparticles. This question of a transition from indirect to direct gap in these nanoparticles will require further exploration.

The effect of the surface and the solvent on the optical properties of colloids of R̂-nc-Ge is another important issue. The similarity in the UV−vis absorption spectra in Figure 6 of R̂-nc-Ge with mean diameters of ∼6.5 nm, but different surface terminations indicate that the nanocrystalline core is mainly responsible for the absorption and that surface effects do not contribute. Figure 7 shows nearly identical UV−vis absorption spectra of the same M̂e-nc-Ge sample in hexane and in methanol. Evaporating the solvent and resuspending the nanoparticles in methanol does not change the UV−vis absorption spectrum. This indicates that solvent effects also do not affect the absorption. Thus, the UV−vis absorption spectra of these colloids reflect the properties of the Ge nanocrystalline core and are largely insensitive to surface and solvent effects. This may

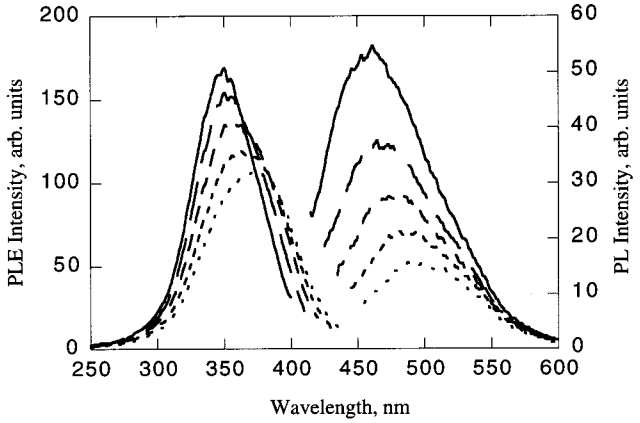

Figure 8. Size-selective PL and PLE of butyl-terminated nanoparticles in hexane with a mean diameter of 6.2 nm. The histogram of these particles appears in Figure 5. The PLE spectra are shown on the left for PL at 410−450 nm, at 10-nm intervals. The PL spectra are shown on the right for excitation at 410−450 nm, at 10-nm intervals. All spectra were recorded with a slit width of 2.5 nm.

indicate the high barrier energy and completeness of the surface termination.

Since the present synthesis produces a continuous size distribution of nanoparticles, the PL and PLE spectra are inhomogeneously broadened. One manifestation of quantum confinement in such a system is a monotonic shift of the PL as the excitation wavelength is changed. This results from the excitation of different sizes of nanoparticles that have different optical transition energies. Similarly, when the detection wavelength is changed, the PLE spectra of the sample should also change monotonically. R̂-nc-Ge produced by this method show optical properties consistent with this model: smaller nanoparticles absorb and emit light at higher energy than the larger nanoparticles. In this case, size selection is solely by changing the excitation wavelength used for PL spectra, or changing the emission wavelength monitored for PLE spectra; no size-selective precipitation, dialysis, or similar techniques were used. Figure 8 shows size-selective PL and PLE spectra of B̂u-nc-Ge with a mean diameter of 6.2 (2.6) nm. The excitation and detection wavelengths were limited to the blue spectral region, although longer wavelength excitation and detection were possible. The continuous shift in both emission and excitation spectra further supports quantum confinement in these B̂u-nc-Ge. Figure 9 shows higher resolution size-selective PL of a toluene colloid of larger M̂e-nc-Ge, with a mean size of 8−10 nm, and shows how far to the red that the PL may be tuned for large nanoparticles. The shrinking of the Stokes shift, the difference in energy between the excitation and PL emission, is also characteristic of quantum confinement. Figure 10 shows size-selective PL spectra of smaller M̂e-nc-Ge, with a mean diameter of ∼3.5 nm. The PL of smaller nanoparticles occurs at higher energy than that of larger particles.

nc-Ge produced by other methods, such as co-sputtering GeO_2 and SiO_2 followed by reduction with H_2, have been reported to photoluminesce at 2.2 eV for 3-nm particles.[6] Nanoparticles produced by our method show intense PL that is broadly tunable from 2 to 4 eV. This higher energy PL suggests strong confinement, unlike

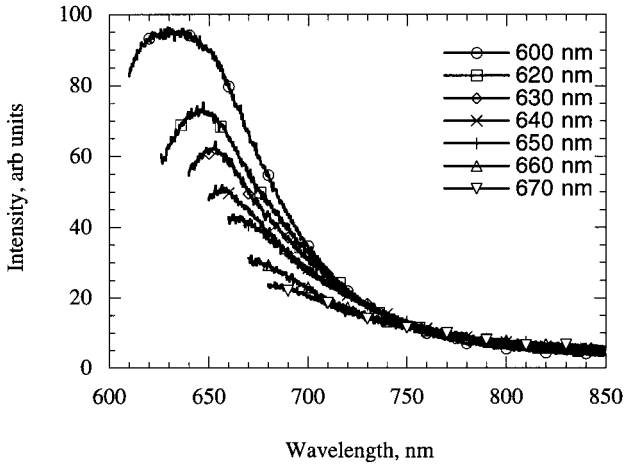

Figure 9. Size-selective PL of methyl-terminated Ge nanoparticles in toluene with a mean diameter of 8−10 nm. The excitation wavelengths are provided in the figure. This PL demonstrates how far to the red PL may be shifted in large nanoparticles. All spectra were recorded with a slit width of 5 nm.

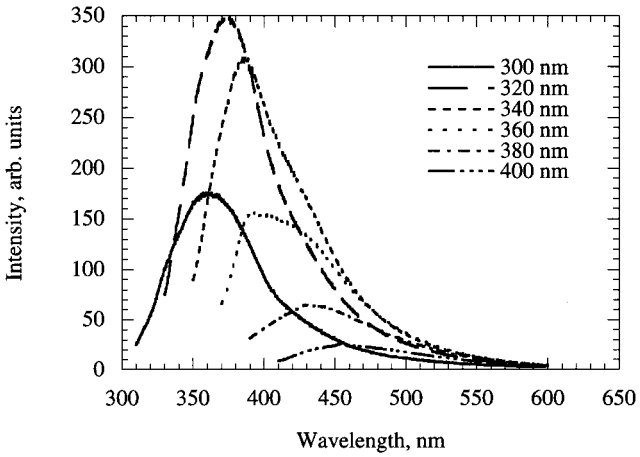

Figure 10. Size-selective PL of methyl-terminated Ge nanoparticles in hexane with a mean diameter of 3.5 nm. The excitation wavelengths are provided in the figure.

nc-Ge produced by other methods. Previous studies of nc-Ge in SiO_2 matrixes did not show monotonic shifts in size-selective spectroscopy. [9−11,56] and may suggest the involvement of traps. In contrast, monotonic shifts are observed from nanoparticles made by this method and there are no obvious strains, interfacial defects, oxides, or impurities to explain the PL. However, the origin of the PL of Ge nanoparticles in an SiO_2 matrix remains an open question. Other groups have made similar materials with different methods and suggested that quantum confinement is responsible for the PL.[5−8,57] Maeda et al. suggested that quantum confinement is responsible for the PL in this system, but found only qualitative agreement between PL spectra calculated from quantum confinement models.[6,57] It was also suggested that PL of films of SiO_2 embedded with Ge nanoparticles prepared by ion implantation results from radiative defect centers in the SiO_2 matrix.[13]

(56) Zacharias, M.; Weigand, R.; Dietrich, B.; Stolze, F.; Bläsing, J.; Veit, P.; Drüsedau, T.; Christen, J. *J. Appl. Phys.* **1997**, *81*, 2384−2390.
(57) Maeda, Y. *Phys. Rev. B* **1995**, *51*, 1658−1670.

Summary

This solution metathesis reaction between $GeCl_4$ and NaGe, KGe, and Mg_2Ge in glyme solvents produces R̂-nc-Ge in useful quantities. There is some provision for size control, by the amounts of starting reagents, or the choice of solvents, although much work remains on controlling the size of the nanoparticles. Examination of the dried colloid by HRTEM shows the presence of crystalline nanoparticles, with the lattice spacing of bulk Ge. However, XRD of the as-prepared colloid showed no diffraction peaks unless heated to the point of breaking the surface alkyl bonds. Powder XRD of the heated powder separated from the colloid revealed nanoparticles in the same size range as HRTEM measurements of the dried colloidal suspensions. FTIR of both the dried colloids and the tan powder showed the termination of the surface of the nanoparticles with alkyls, and repeated heating to 100 °C in air demonstrated that the surface alkyl groups effectively protect the nanoparticles from surface oxidation. The UV−vis absorption, PL, and PLE spectra of the colloids do not change significantly with solvent or surface termination, indicating that the nanocrystalline core is largely responsible and that solvent or surface effects do not contribute significantly. The size-selective PL and PLE spectra of the colloids formed by the nanoparticles in both nonpolar and polar solvents shift monotonically, consistent with quantum confinement rather than defects or impurities. Additionally, the PL of smaller nanoparticles occurs at a higher energy than those of larger nanoparticles, and colloids with a large size distribution show broadly tunable emission. Further work incorporating size-selected precipitation techniques, and low-temperature lifetime and photoluminescence spectroscopy is in progress.

Acknowledgment. We thank the staff at the National Center for Electron Microscopy, particularly Chris Nelson for useful discussion and assistance with the HRTEM. We also thank Roar Kilaas and John Turner for help with the interpretation of the HRTEM images. Work at NCEM was performed under the auspices of the Director, Office of Energy Research, Office of Basic Energy Science, Materials Science Division, U.S. Department of Energy under Contract DE-AC-03-76SF00098. This work was supported by the National Science Foundation (DMR-9505565, DMR-9803074) and the Campus Laboratory Collaboration Program of the University of California. Work at the Lawrence Livermore National Laboratory was supported by the Laboratory Directed Research and Development program and was performed under the auspices of the U.S. Department of Energy under Contract W-7405-ENG-48.

CM990203Q